Validation of an efficient and robust MRI-guided radiotherapy planning approach for targeting abdominal organs and tumours in the mouse.

Veerle Kersemans[1], John S Beech[1], Stuart Gilchrist[1], Paul Kinchesh[1], Philip D Allen[1], James Thompson[1], Ana L Gomes[1], Zenobia D'Costa[1], Luke Bird[1], Iain DC Tullis[1], Robert G Newman[1], Abul Azad[1], Ruth J Muschel[1], Borivoj Vojnovic[1], Mark A Hill[1], Emmanouil Fokas[1], and Sean C Smart[1]

[1]*CRUK/MRC Oxford Institute for Radiation Oncology, University of Oxford, Oxford, United Kingdom*

Synopsis

The aim was to develop and validate a robust and accurate method of MR-IGRT delivery to abdominal targets in the mouse that takes advantage of the strengths of each of its components: MRI for soft tissue contrast and target identification, CBCT for accurate dose calculation and IGRT for accurate, collimated X-ray beam delivery. A multimodality cradle was developed and evaluated to enable transfer of the mouse between MR and the IGRT platform. Additionally, each step of the MG-IGRT process was validated, both in vitro using BANG gel dosimeters and in vivo by targeting the adrenal glands in mice.

Purpose

CT-guided radiotherapy (RT) platforms are commercially available but the images show poor soft tissue contrast, hindering applications in the body. Invasive workarounds have been proposed[1] but these do not provide a general solution to the problem. We validate the use of apparatus and a workflow[2] that provides a general solution for enabling MRI to be used in RT planning with application in the mouse body as previously described[3].

Methods

MRI was performed at 7T (Varian) using appropriately sized quadrature birdcage RF coils (Rapid Biomedical). MR-guided RT (MR-IGRT) was performed on the Small Animal Radiation Research Platform (XStrahl). A custom made cradle was developed to enable transfer of the mouse between MR and the IGRT platform without introduction of large-scale body deformations. Rotationally asymmetric BANG gel dosimeters (n=5) were irradiated with 2 intersecting, orthogonally-applied 2-4mm wide rectangular x-ray beams in order to present an MR-visible but CT-invisible target. This gel was imaged by MRI using a CE-FAST scan at 273µm isotropic resolution. The gel was transferred to the IGRT system and a CT image was produced at 160µm resolution. The MR and CT images were registered using a finite iterative closest point algorithm. Next, a conical arc beam was applied with its centre-of-rotation at the manually-defined centre of the beam-intersection as defined by the registered MR-CT image. MRI was repeated to allow assessment of the MR-IGRT beam delivery and the offset between the target and the delivered beam was used to measure targeting accuracy. Long term movements of mice were assessed by repeated MRI of the same mouse when held in a non-moving cradle (to define the intrinsic body motions), and also by repeated imaging of the same mouse as it was transferred between the MR and CT systems (to define the extrinsic motions induced through movement of the cradle and mouse). A respiration-gated, constant TR, bSSFP scan (TE 1.134ms, TR 3.268ms, FA 15˚, 16µs hard pulse, resolution 400µm isotropic, 0˚/180˚ RF phase alternation) was used. Confirmation of accuracy of beam delivery was assessed in vivo in 4 mice, by targeting one adrenal gland with a single RT beam. The same bSSFP scan was used, the animal was transferred to the IGRT system and a CT image was produced with a total procedure time of below 30 minutes per mouse. MR-to-CT registration was performed using the deformable MIND registration technique[4], the adrenal was identified on the MR-CT image, and the RT beam (10Gy) was delivered using adrenal-size-matched collimators. Animals were killed at 30 minutes post irradiation and the adrenals and adjacent kidneys were prepared for γH2AX and DAPI staining to assess the DNA damage induced by the x-ray beam.

Results and Discussion

The MR image of a BANG gel featuring the intersecting beam for targeting is shown in Fig1A, and the same gel, following MR-IGRT is shown in Fig1B. A mean offset between target- and result-centres of 0.56±0.18mm (n=5) was measured. The intrinsic body motions were dominated by peristalsis and body droop, the latter having a maximum excursion of approximately 0.5mm over 30 minutes. The extrinsic motions, measured after 5 transfers between the MR and RT systems, were measured to be ca. 0.5mm, approximately the same as the underlying error demonstrated by the BANG gel targeting and intrinsic motion tests. bSSFP MR allowed for fast imaging of the mouse abdomen (<10 minutes from anaesthesia induction to transfer to RT) and the adrenals could be easily localised on MR (Fig2A), but not on CT (Fig2B). The registered MR-CT image (Fig2C) was successfully used to guide RT delivery of 10Gy to one of the adrenals (Fig2D) as confirmed by γH2AX staining (Fig3). In the irradiated adrenals (Fig3AB) the DNA damage was abundant and homogenously distributed while background levels of DNA damage were seen in the kidney proximal to the collimated irradiation (Fig3C) or in the non-irradiated adrenal (Fig3D). Any failure in any part of the MR-IGRT procedure would have resulted in an absent or partial distribution of the γH2AX foci in the MR-IGRT targeted adrenal glands. The entire Mr-IGRT procedure was fast, <30 minutes per mouse, and through the use of 2 cradles 2 mice could be run simultaneously, one in the MR system, one in the IGRT system, to give an effective turnaround time of <15 minutes per mouse.

Conclusions

The proposed MR-IGRT method presents a general solution to enabling robust, accurate and efficient targeting of organs and, by inference tumours, in the mouse and can operate with a sufficiently high throughput to allow fractionated treatments to be given routinely.

Acknowledgements

The work presented was supported financially by Cancer Research UK (CRUK grants C5255/A12678, C2522/A10339), the Engineering and Physical Sciences Research Council (EPSRC grant C2522/A10339) and the Medical Research Council Unit Grant for the Oxford Institute for Radiation Oncology. The authors also acknowledge expert technical assistance from the Institute Mechanical and Electronics Workshops,

animal facilities team and anyone else who contributed financially or in kind.

References

1. Thorek DL, Kramer RM, Chen Q, Jeong J, Lupu ME, Lee AM, et al. Reverse-Contrast Imaging and Targeted Radiation Therapy of Advanced Pancreatic Cancer Models. Int J Radiat Oncol Biol Phys. 2015;93(2):444-53.

2. J. Beech, D. Allen, J. Thompson, S. Gilchrist, P. Kinchesh, R. et al. MR-guided radiotherapy planning in the mouse abdomen Magn Reson Mater Phy (2015) 28 (S1): S336.

3. Corroyer-Dulmont A, Falzone N, Kersemans V, Thompson J, Hill M, Allen PD, et al. MRI-Guided Radiotherapy of the SK-N-SH Neuroblastoma Xenograft Model Using a Small Animal Radiation Research Platform. Br J Radiol. 2016:20160427.

4. Heinrich MP, Jenkinson M, Bhushan M, Matin T, Gleeson FV, Brady SM, et al. MIND: modality independent neighbourhood descriptor for multi-modal deformable registration. Med Image Anal. 2012;16(7):1423-35.

Figures

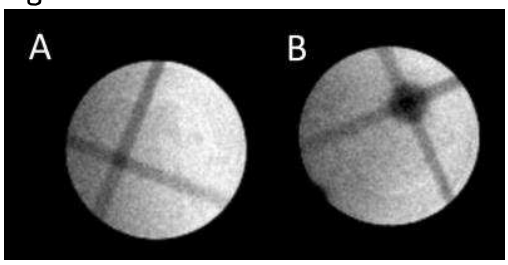


Fig. 1: MR-IGRT of a painted feature in a BANG gel. (A) A target volume was created by a pair of orthogonal 2 mm diameter rectangular beams and (B) targeted following MR-IGRT using a conical arc, delivered at a 45 degree oblique angle and using a 5 mm round collimator.

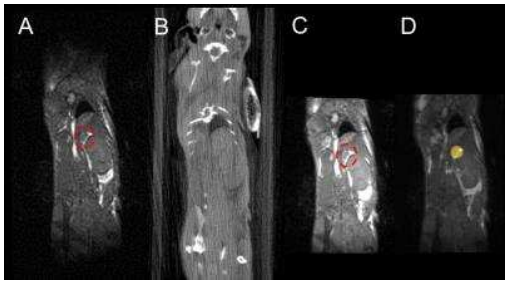


Fig. 2: In vivo MR-IGRT of the adrenal glands. (A) respiratory-gated bSSFP MR; (B): RT planning CBCT; (C) CBCT-MR to guide the RT treatment delivery; (D) treatment plan for the adrenal.

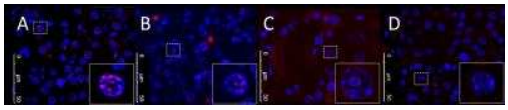


Fig. 3: Fluorescent images of p-γH2AXSer139 (red) counterstained with DAPI (blue) to visualise the nucleus. Images were acquired for 2 regions within the irradiated adrenal (A, B), the kidney area proximal to the irradiated adrenal (C) and the non-irradiated contralateral adrenal (D). Representative images are shown.